

Scattering of ^{28}Si from ^{208}Pb

P. R. Christensen, S. Pontoppidan, and F. Videbaek

Niels Bohr Institute, University of Copenhagen, DK-2100 Copenhagen Ø, Denmark

J. Barrette,* P. D. Bond, Ole Hansen, and C. E. Thorn

Brookhaven National Laboratory, Upton, New York 11973

(Received 20 September 1983)

Elastic and inelastic scattering of ^{28}Si on ^{208}Pb have been investigated at 209.8 MeV with high resolution. The angular distributions can be well described by coupled channel calculations when the ion-ion potential has a diffusivity of 0.65 fm. Deformation lengths extracted are in good agreement with those obtained from analysis of light ion reaction data.

I. INTRODUCTION

In a previous Letter,¹ high resolution measurements of elastic and inelastic scattering of 695 MeV ^{86}Kr from ^{208}Pb were reported. A coupled channels analysis demonstrated that the data could be described by a potential with a real part equivalent to the global potential of Refs. 2 and 3, in contrast to optical model analyses of scattering data with inferior resolution.^{4,5} The present measurements and analyses complement the earlier ones in two aspects: First, a projectile (^{28}Si) with large deformation (≈ -0.37) was used, while ^{86}Kr supposedly is spherical, and second, the unambiguous observation of the $0^+ \rightarrow 2.62$ MeV 3^- transition in ^{208}Pb allows a more critical test of the reaction model. As a result, more detailed information on the scattering potential could be obtained. The data of Ref. 1, which were described with a potential of diffusivity $a = 0.50$ fm, are quite insensitive to the value of a . The present, more probing, data demand a larger value, $a \approx 0.65$ fm. Finally, a comparison of deformation lengths derived from inelastic scattering to $^{28}\text{Si}(2^+)$ with projectiles from ^4He to ^{208}Pb is presented.

II. EXPERIMENT AND RESULTS

The 209.8 MeV ^{28}Si beam was produced by the BNL double tandem accelerator and the targets were $48 \mu\text{g}/\text{cm}^2$ ^{208}Pb enriched to 98.7% on $10 \mu\text{g}/\text{cm}^2$ carbon backings. The scattered particles were analyzed in a quadrupole-dipole-dipole-dipole (QDDD) magnetic spectrometer and detected and identified by a two-volume gas proportional focal plane detector. The spectrometer aperture was 100×120 (mrad)² for the three most backward angles, and 40×120 (mrad)² elsewhere, where the smaller angle is in the reaction plane. The accuracy of the angle setting was ≤ 3 mrad. By matching beam and spectrometer optics an energy resolution of ≈ 150 keV was achieved and the elastic scattering as well as the inelastic transitions to $^{28}\text{Si}(1.78 \text{ MeV}, 2^+)$, $^{208}\text{Pb}(2.62 \text{ MeV}, 3^-)$, and $^{208}\text{Pb}(4.08 \text{ MeV}, 2^+)$ were identified. At the most backward angles a broad structure appears above the 4.08 MeV groups (see Fig. 1), corresponding in energy to mutual excitation of $^{28}\text{Si}(2^+)$ and $^{208}\text{Pb}(3^-)$ ($Q = -4.40$ MeV) and excitation of

the $^{28}\text{Si}(4.62 \text{ MeV}, 4^+)$ state. Several levels in ^{208}Pb can also contribute to this structure, and therefore no detailed analysis of it was attempted. The Si-ion charge state distribution was measured at forward and backward angles for elastic scattering; the percentage of charge-state 13 ions (which were recorded in all other measurements) did not change within the statistics ($< 5\%$) of the measurements. The angular distributions of the differential cross sections measured for the various transitions are shown in Fig. 2.

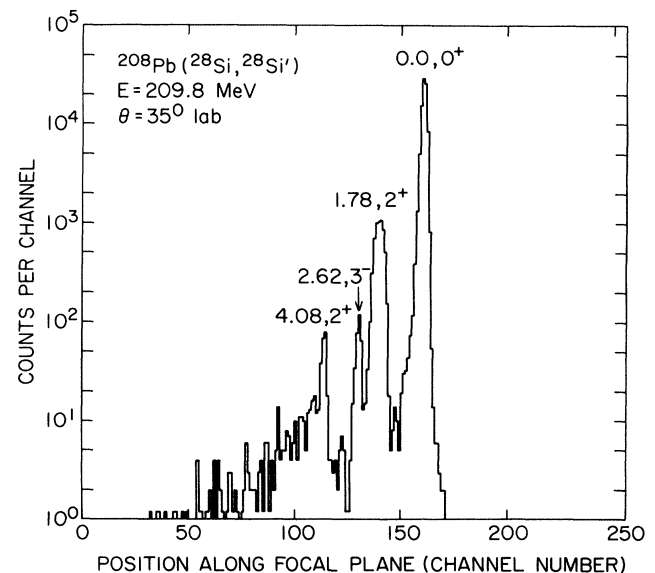


FIG. 1. Spectrum of $^{208}\text{Pb}(^{28}\text{Si}, ^{28}\text{Si}')$ (for charge state 13) at 35° laboratory scattering angle and an incident energy of 209.8 MeV. Number of counts per channel are plotted against channel number, where the latter represents distance along the focal plane of the spectrometer. The 1.78 MeV ^{28}Si excitation (noted as 1.78, 2^+) is broadened by the recoil effects from the in-flight gamma decay of the excited Si nuclei. The inelastic ^{28}Si group corresponding to excitation of the $^{208}\text{Pb}, 5^-$ state at 3.20 MeV would be situated near channel 125 in the spectrum. With the currently obtained counting statistics, this transition could not be positively identified.

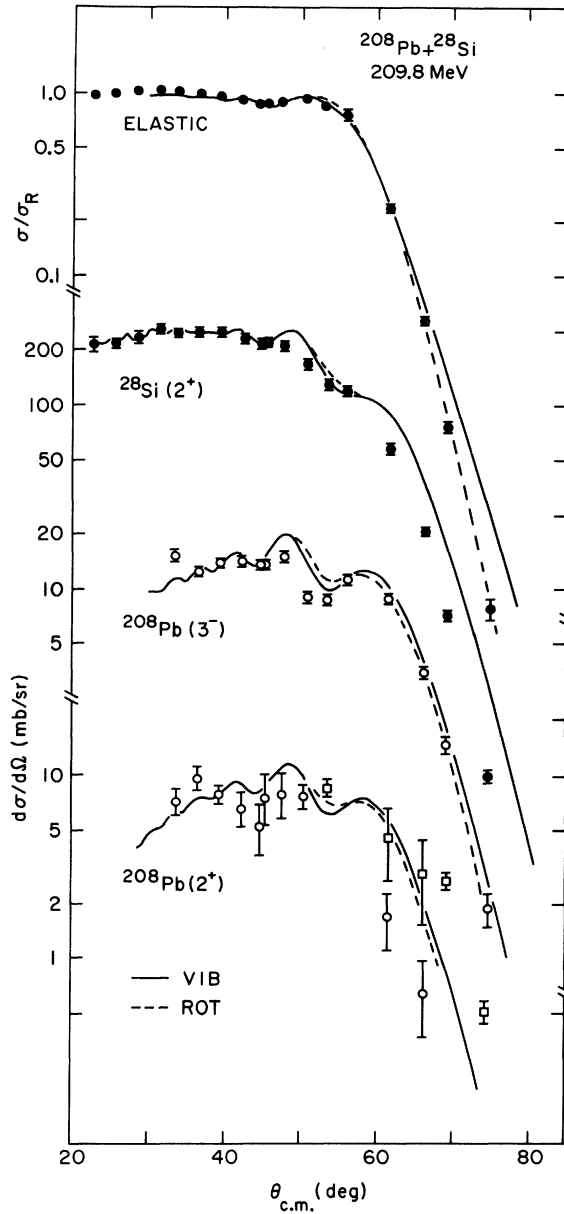


FIG. 2. Cross section angular distributions in the center of mass system. The top (filled circles) represents elastic scattering divided by the Rutherford value. The second data set (also filled circles) is for the ^{28}Si , 1.78 MeV, 2^+ excitation. The third set (open circles) corresponds to the ^{208}Pb , 2.62 MeV, 3^- transition, while the angular distribution at the bottom is for the ^{208}Pb , 4.08 MeV 2^+ state. At back angles, two sets of data are given for this transition. The open squares correspond to all counts from 4.08 MeV of excitation to about 4.3 MeV, and thus cover part of the complex group near the $\text{Si}(2^+) + \text{Pb}(3^-)$ mutual excitation. The open circles correspond to the region very close to 4.08 MeV, with a range extrapolated from the well-defined 2^+ group at more forward angles. The curves are coupled channels results as explained in the text.

III. ANALYSIS

The analysis was made with the coupled channels (CC) codes QUICC (Ref. 6) and VAX-CHUCK. The latter is a ver-

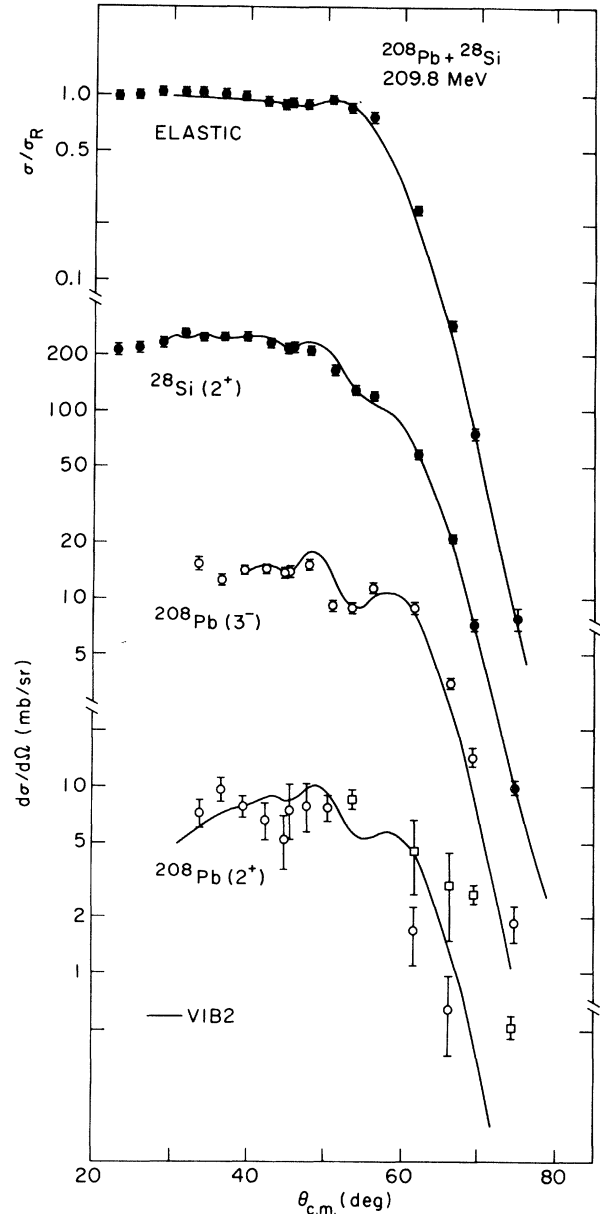


FIG. 3. Data and notation as in Fig. 2. The curves are CC calculations using the vib2 parameters of Tables I and II. See the text for further details.

sion of code CHUCK-3 (Ref. 7) modified for partial-wave interpolation of the S matrix.⁸ QUICC was used for optical parameter searching and for other exploratory calculations, while VAX-CHUCK was employed in the final calculations, which included more channels. All calculations included Coulomb excitation, and 500 partial waves were used. The nuclear form factors were integrated out to a distance of 20 fm, while the Coulomb form factor was integrated to 120 fm. The integration step length was 0.05 fm.

Two different models for the nuclear form factors, called vibrational and rotational, were used in the calculations. In the vibrational model the deformed scattering potential was expanded to first order in the relevant defor-

TABLE I. Scattering and coupling potentials. The potentials were of the form

$$U(r) = (-V - iW) \left[1 + \exp \frac{r-R}{a} \right]^{-1} + V_{\text{Coul}},$$

with $R = r_0(28^{1/3} + 208^{1/3})$. The Coulomb radius was $R_c = r_{0c}(28^{1/3} + 208^{1/3})$ and the deformation lengths in the vibrational calculations (see also the text and Table II) were $\beta_\lambda R_A$, $R_A = r_0 A^{1/3}$, where A is the baryon number of the excited nucleus.

Label	V (MeV)	r_0 (fm)	a (fm)	W (MeV)	r_{0c} (fm)
vib1	40	1.30	0.50	25	1.32
rot	40	1.28	0.50	25	1.32
vib2	40	1.248	0.65	25	1.32

mation parameter. The ^{208}Pb $0^+ \leftrightarrow 3^-$ and $0^+ \leftrightarrow 2^+$ transitions were included, together with the ^{28}Si 2^+ channel. Reorientation was taken into account for the ^{28}Si (1.78 MeV, 2^+) state which has a positive quadrupole moment with a magnitude⁹ close to the rotational value.

In the rotational scheme, the ^{28}Si excitations were described by expanding the deformed potential on spherical harmonics and projecting the quadrupole part out. The $0^+ \leftrightarrow 2^+ \leftrightarrow 4^+$ transitions of the Si ground state band, as well as reorientation for the 2^+ state, were included in the calculations. The ^{208}Pb excitations, $0^+ \leftrightarrow 3^-$ and $0^+ \leftrightarrow 2^+$, were treated as in the vibrational scheme.

The potential used initially for the vibrational calculations was similar to that used in the $^{86}\text{Kr} + ^{208}\text{Pb}$ analysis of Ref. 1 (Table I, vib1), while the rotational results were obtained from a slightly different potential (rot of Table I).

Calculations with these potentials are shown in Fig. 2. The coupling strengths are displayed in Table II. The vibrational calculation (fully drawn curve) fits the Pb 2^+ and 3^- data well, but fails in the elastic channel to follow the slope of the falloff from Rutherford scattering at the

angles backwards of the Coulomb-nuclear interference region. Similarly, the calculations for the Si 2^+ channel overpredict the Coulomb-nuclear interference effects and the backward angle cross section. The rotational calculation (dashed curve in Fig. 2) gives a better account of the elastic channel but is otherwise very similar to the vibrational calculation.

Attempts to improve the agreement between CC calculations and the data by varying r_0 or a in the scattering potential were unsuccessful, as were variations of $\beta_2 R_{\text{Si}}$ combined with variations of r_0 .

A substantial improvement in the fit quality was obtained by a correlated variation in r_0 , a , and $\beta_2 R_{\text{Si}}$. r_0 and a were changed in such a way that potentials of different (r_0, a) values intersect the original potential at the "point of sensitivity" as defined in Refs. 2 and 3, and as discussed for $^{86}\text{Kr} + ^{208}\text{Pb}$ in Ref. 1. For increasing a , $\beta_2 R_{\text{Si}}$ had to be decreased. The final results for the vibrational scheme are shown in Fig. 3 and the corresponding potential parameters and coupling strengths (labeled vib2) are given in Tables I and II, respectively. The calculations shown in Fig. 3 agree well with the data and represent a distinct improvement over the calculations shown in Fig. 2. A similar procedure may be applied in the rotational scheme, leading to equivalent results.

IV. DISCUSSION AND CONCLUSIONS

The present data are more detailed and more sensitive to the geometry of the scattering potential than the previous $^{86}\text{Kr} + ^{208}\text{Pb}$ results¹ and than an earlier $^{28}\text{Si} + ^{208}\text{Pb}$ experiment at lower bombarding energy.¹⁵ The analysis shows that in order to describe the inelastic scattering to the strongly coupled 2^+ state in ^{28}Si , a potential with a larger diffusivity than used in Ref. 1 is needed, while the elastic scattering alone can be described equally well by potentials with smaller diffusivities as long as they have the same point of sensitivity. The present potential, vib2, is very close to the folding estimate of Ref. 15, which is equivalent in a range 11–16 fm to a Woods-Saxon poten-

TABLE II. Inelastic coupling matrix elements. All electric coupling matrix elements used in the Si + Pb analysis are from the literature, as quoted in the table. They do not necessarily correspond to a β_{Coul} that is equal to the nuclear β value. The labels "vib" and "rot" in the table headings refer to the vibrational and rotational schemes of the coupled channels analysis, as explained in the text. The sign for $\beta_2 R_{\text{Si}}$ in the vibrational case indicates that reorientation was used at the rotational value, assuming a negative deformation (positive quadrupole moment). The accuracy of any quoted βR value is probably not better than $\pm 15\%$.

State	$\langle \lambda \mathcal{M}(E\lambda) 0 \rangle$ $e \text{ fm}^\lambda$	$\beta_\lambda R_A$ (fm)					
		Si + Pb vib1	Si + Pb vib2	Si + Ni vib	α or p vib	Si + Pb rot	(α, α') rot
^{28}Si							
1.78 MeV, 2^+	-18.06	-1.23	-1.06	-1.37	(-).121	-1.20	-1.25
^{208}Pb							
2.62 MeV, 3^-	815	0.56	0.56		0.87	0.55	
^{208}Pb							
4.08 MeV, 2^+	55	0.43	0.43		0.42	0.42	
References	9, 11, 12	Present work	Present work	10	13, 11, 14	Present work	16

tial with parameters $V=35$ MeV, $r_0=1.25$ fm, and $a=0.63$ fm.

The analysis also demonstrates that for ^{28}Si scattering the rotational and vibrational form factor recipes lead to closely equivalent results and the data do not distinguish between the two procedures. Inspection of the form factors of the two models shows that the shapes are essentially the same and that one can obtain nearly identical form factors by allowing small changes of radii and deformation lengths.

Values of $\beta_2 R_{\text{Si}}$, when ^{28}Si is excited by ^4He and ^{60}Ni , are also included in Table II. From folding¹⁷ and proximity¹⁸ model estimates, one would expect the deformation lengths to decrease by about 30% for projectiles from ^4He to ^{208}Pb . Within the uncertainties on the $\beta_2 R_{\text{Si}}$ values they are constant, although if one stretches the uncertainties the predicted variation can be accommodated.

Also included in Table II are βR_{Pb} values for ^4He excitation of the ^{208}Pb 3^- state and ^1H excitation of the ^{208}Pb 2^+ state. The first value shows a decrease in βR for Si

over ^4He , while the latter value is constant.

The tentative conclusion with respect to βR values is that at least for $\lambda=2$, one can derive nuclear coupling strengths for heavy ion inelastic scattering that agree with light ion values.

The specific sensitivity of the inelastic scattering to the diffusivity implies that the potential is not probed merely at a single distance, but rather over a range of distances, somewhat in contrast to previous analyses (see, e.g., Refs. 1, 3, 19, and 20).

ACKNOWLEDGMENTS

The authors are indebted to A. Baltz for many illuminating discussions and for the use of his coupled channels code QUICC. This research was supported by the Danish National Science Research Council and by the U. S. Department of Energy under Contract No. DE-AC02-76CH00016 with BNL.

*Present address: CEN de Saclay, 91191 Gif-sur-Yvette Cedex, France.

¹Jiang Cheng-Lie *et al.*, Phys. Rev. Lett. **47**, 1039 (1981).

²P. R. Christensen and A. Winther, Phys. Lett. **65B**, 19 (1976).

³R. A. Broglia and A. Winther, *Heavy Ion Reactions* (Benjamin/Cummings, Reading, Mass., 1981), Vol. 1.

⁴J. R. Birkelund *et al.*, Phys. Rev. C **13**, 133 (1976).

⁵R. Vandenbosch *et al.*, Phys. Rev. C **13**, 1893 (1976).

⁶A. J. Baltz, Phys. Rev. C **25**, 240 (1982).

⁷P. D. Kunz (unpublished).

⁸Code CHUCK-3 was modified to run on a VAX-780 computer with partial wave interpolation by B. S. Nilsson and F. Videbaek.

⁹P. Endt and C. van der Leun, Nucl. Phys. **A310**, 1 (1978).

¹⁰P. D. Bond *et al.*, Phys. Lett. **114B**, 423 (1982).

¹¹J. S. Lilley, M. A. Franey, and D. H. Feng, Nucl. Phys. **A342**, 165 (1980).

¹²J. F. Ziegler and G. A. Peterson, Phys. Rev. **165**, 1337 (1968); M. Sasao *et al.*, Phys. Rev. C **15**, 217 (1977).

¹³K. van der Borg *et al.*, Nucl. Phys. **A365**, 243 (1981).

¹⁴A. Scott and M. P. Fricke, Phys. Lett. **20**, 654 (1966).

¹⁵J. S. Eck, T. R. Ophel, P. D. Clark, D. C. Weisser, and G. R. Satchler, Phys. Rev. C **23**, 228 (1981).

¹⁶M. Rebel *et al.*, Phys. Rev. Lett. **26**, 1190 (1971).

¹⁷P. J. Moffa, C. B. Dover, and J. P. Vary, Phys. Rev. C **16**, 1857 (1977).

¹⁸A. J. Baltz and B. F. Bayman, Phys. Rev. C **26**, 1969 (1982).

¹⁹N. K. Glendenning, in *Proceedings on the International Conference on Reactions Between Complex Nuclei, Nashville, 1974*, edited by R. L. Robinson, F. K. McGowan, J. B. Ball, and Y. H. Hamilton (North-Holland, Amsterdam, 1974), Vol. II, p. 137.

²⁰G. R. Satchler, see Ref. 19, p. 171.